Characterization of a strain-inducing defect in CdTe by magnetoluminescence spectroscopy

L. Worschech, W. Ossau, and G. Landwehr
Physikalisches Institut der Universität Würzburg, 97074 Würzburg, Germany
(Received 17 May 1995)

On the basis of the magnetoluminescence spectroscopy of a new isoelectronic defect complex in indium-doped CdTe the local structure and the associated strain direction are identified. This strain-inducing complex has a tetrahedral structure consisting of two substitutional indium atoms, one cadmium vacancy, and another cadmium atom. The Zeeman-effect experiments on the low-temperature photoluminescence are discussed in terms of a modified effective Hamiltonian. It is shown that the symmetry of the exciton binding trap is lower than trigonal. The bound exciton line at 1.584 19 eV (C line) is found to be associated with this complex and dominates the photoluminescence (PL) spectra in indium-doped CdTe. As many as 28 magnetic subcomponents in the PL spectra of the C line are resolved when the anisotropy of the Zeeman splitting is investigated. A modified perturbation Hamiltonian has led to an excellent agreement with the observed data. The C line is interpreted as a superposition of bound exciton recombinations from several inequivalent sets of tensionally strained defects with an angle of inclination $\tau=2°$ with respect to the trigonal [1,1,1] axis. The conduction-band g factor $g_e=-1.73$ and the valence-band parameters $K=0.75$, $L=0.0$ and the additional strain constant ratio $W/D=-1.1$ are to our knowledge the first values of this kind published for an isoelectronic trap with low symmetry. In zero magnetic field, the bound exciton recombinations from the inequivalent defects coincide, resulting in a luminescence line with only 0.12 meV half-width. We interpret the temperature quenching of the total emission intensity as a consequence of strain, induced by the defect complexes.

I. INTRODUCTION

II-VI semiconductors have been intensely investigated in the past decade. Although II-VI materials have been known for a long time, our knowledge of their physical properties is not nearly as complete as for III-V semiconductors. One of the reasons is the frequent difficulty in producing wide-gap materials like ZnSe, with n-type as well as p-type conductivity. In addition, it is not easy to achieve carrier concentrations above 10^{18} cm^{-3}. It is well known that self-compensation can occur, and that an increase of dopants can in fact cause a decrease of the free-carrier concentration. Usually such self-compensation effects are attributed to defect complexes consisting of chemical dopants in conjunction with vacancies.

A II-VI material of special interest is CdTe. It has a band gap not too different from that of GaAs. Due to the ionicity of its chemical bond it has an electrooptical coefficient (which relates the change in refractive index by an electric field) about four times as large as in GaAs. Thus CdTe is a promising material for electro-optical modulators. On the other hand, it is known that the mechanical hardness of CdTe is considerably less than that of GaAs. An unusual property of CdTe is that its luminescence may degrade with time.[1] This has been explained qualitatively by relaxation effects connected to defects in CdTe. Whereas some defects can be attributed to chemical impurities on lattice sites, a large number of them have been connected with defect complexes. For their investigation, photoluminescence (PL) spectroscopy has been widely used. However, in most cases a reliable identification of the physical origin of the defects has been impossible. The so called C line at an energy of 1.584 19 eV has been attributed to a defect complex. In crystals of good quality the line has a width of 1 meV or less. It has been proposed that this is connected with an exciton bound to an isoelectronic defect consisting of two In atoms on Cd sites and a Cd vacancy. This has been demonstrated by luminescence investigations of Cd films grown by molecular-beam epitaxy (MBE).[2] With this technique the Cd vacancy concentration and the In doping can be varied in a controlled manner. However, details of the complex have not been known up to now.

By measuring the Zeeman splitting of luminescence lines, originating from isoelectronic defects, it is possible to obtain detailed information about the symmetry of defects. This has been demonstrated for isoelectronic defects in GaP.[3] However, the observed lines are usually broadened due to sample inhomogeneity or internal strain gradients to such an extent that the potential of the method could not fully be exploited. Recently we undertook a study of relaxation effects in CdTe by studying the magnetoluminescence of the C line. The quality of MBE layers grown on CdTe substrates in our laboratory has reached such a level that detailed studies have become possible. In a bulk crystal of high perfection we observed a C line with unusual sharpness. A half-width of only 0.12 meV allowed the observation of as many as 28 Zeeman components in a high magnetic field. In order to exploit fully the magnetoluminescence technique, we investigated the anisotropy of the Zeeman splitting in small angular steps. The analysis of the experimental data showed, however, that the type of spin Hamiltonian which has been employed so far to interpret magneto-

0163-1829/95/52(19)/13965(10)/$06.00

optical data was insufficient to explain our findings. Consequently we modified the usual Hamiltonian so that we can offer a detailed model for the complex causing the C line.[4]

In Sec. II the samples investigated are described as well as the experimental method. After the analysis of the experimental data, a detailed model for the complex is proposed, which is in quantitative agreement with the anisotropy of the observed Zeeman splitting. The model involves three nearest neighbors in a (1,1,1) plane; that is, two In atoms at Cd sites and an adjacent Cd vacancy. The nearest Cd atom in the [1,1,1] direction is tilted by 2°. Furthermore we will analyze the behavior of the temperature-dependent luminescence intensity and the coupling to the acoustical phonon sideband with respect to our defect complex model.

II. EXPERIMENT

A. Sample preparation

We investigated In-doped bulk CdTe grown by the Bridgman method by II-VI-Incorporation, Saxonburg (USA), and In-doped CdTe films grown by molecular-beam epitaxy (MBE) in our institute. The 1-μm-thick layers have been produced on undoped (001) CdTe substrates. In order to investigate the Zeeman effect and resolve the magneto-optical transitions, sharp lines are essential. In different samples the intensity as well as the half-width of the C line vary. We found C-line half-widths to range from 0.12 to 1.0 meV. After etching a bulk sample with a bromine-methanol solution and thus removing an upper layer of about 1-μm thickness, we found a C line with a 0.12-meV width. However, after letting the sample sit for a few weeks the Zeeman splittings were impossible to detect. We observed a drastic change in the photoluminescence with time, resulting in a broadening of the C line. This aging effect starts at the surfaces and proceeds into the CdTe sample.

B. Experimental procedure

Photoluminescence (PL) was excited with the 514-nm line of an argon-ion laser. The spectra were measured with a single-grating 1-m spectrometer and a cooled photomultiplier. For the Zeeman-effect measurements a superconducting split coil magnet with a maximum field of 7.5 T was employed, and the spectra were recorded in the Voigt configuration. The samples were rotated in small steps of 5° from **B**, the magnetic field, along the [1,1,0] to [0,0,1] axes, **B** lying oriented always in a (1,1,0) plane. The sample temperatures could be varied between $T=1.7$ and 300 K.

III. EXPERIMENTAL RESULTS

The doping of CdTe samples with indium usually results in material with high resistivity contrary to the expected n-type conductivity. In the PL spectrum the C line appears, and the intensity of the other usual bound exciton transitions is weak. The strong correlation of the C line with Cd vacancies has been shown by varying the Cd flux in MBE-grown indium-doped samples. Thus the C line in PL spectra clearly indicates self-compensation.[2]

The luminescence spectrum for a bulk sample heavily doped with indium is shown in Fig. 1. The prominent C line with an energy of 1.584 19 eV is very sharp and accompanied by a phonon-induced shoulder at the low-energy side. The line at 1.589 28 eV can be attributed to an exciton bound to an indium donor. The third, weak line can be identified as an exciton bound to a copper acceptor. Spectra of this kind were observed both for MBE layers of about 1-μm thickness (grown as CdTe substrates) as well as for bulk samples.[5–8]

For bulk materials we observed that the C line exhibits an increase of the half-width and a decrease in intensity by a factor of 5 in a period of half a year. However, etching these samples with a bromine-methanol solution and thus removing the surface layers restores the sharpness and intensity of the line. Obviously the bulk defect complexes are not affected by this aging effect. Two PL spectra of a MBE-grown CdTe sample are depicted in Fig. 2. Spectrum (a) was measured immediately after the growth of the sample. The intensity of the acoustical-phonon sideband with a maximum in the TA(X) phonon is more than 50% of the C-line intensity. For the same sample the C line was not detectable in the PL spectrum (b) after one month storage at room temperature.

The assignment of the C-line luminescence to the

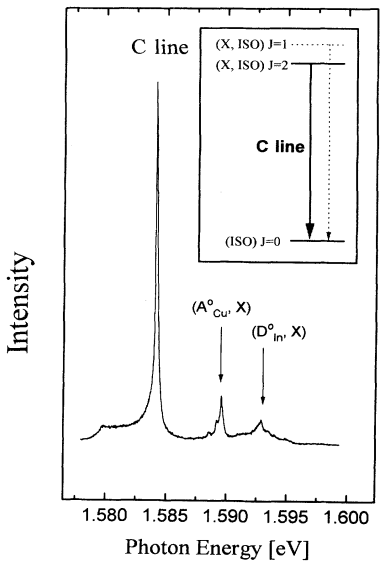

FIG. 1. Photoluminescence (PL) spectrum of a highly indium doped CdTe sample detected for $T=1.7$ K without magnetic field. The C line with the typical low-energy phonon sideband dominates the photoluminescence spectrum. Because of the orientational degeneracy at zero magnetic field, the high number of magnetic subcomponents are coincident in the sharp luminescence C line with a 0.12-meV half-width. The lines for higher energies are related to recombinations from excitons bound to the copper, nitrogen, and silver acceptors and to some donors.

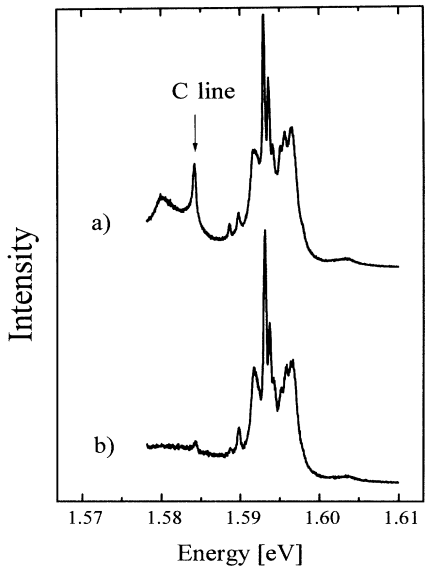

FIG. 2. PL spectra of a MBE-grown CdTe film. Spectrum (a) was detected immediately, and (b) one month after the growth of the sample. The C line disappears with time in the PL spectra of MBE-grown CdTe films.

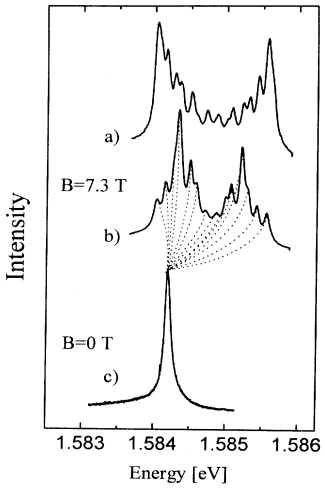

FIG. 3. Low-temperature photoluminescence spectra of an indium-doped bulk CdTe sample. With magnetic field **B** in Voigt geometry for polarization parallel (a) to a [110] plane and (b) perpendicular to a [110] plane. The orientation of **B** is 15 rotated in the [110] plane from the (110) axis. Photoluminescence spectrum (c) shows that all magnetic subcomponents of the C line are degenerate in the C line for $B=0$ T.

isoelectronic complex In_{Cd}-V_{Cd}-In_{Cd} is confirmed by the observed strong anticorrelation of the C-line intensity with the Cd flux in MBE-grown[2] CdTe layers. With increasing Cd flux the oscillator strength of the C line decreases, and the mobility and concentration of the charged carriers are enhanced strikingly. No additional line in the PL spectra is related to the C line. The absence of two particle transitions, for instance the donor-acceptor pair recombination,[9] supports the concept of an isoelectronic state. Therefore, we exclude an acceptorlike or donorlike impurity center to be associated with the C-line luminescence.

Because of the site spectroscopy T_d the electronic states of bound excitons are orientationally degenerate. One orientation of the defect complex has preference for further considerations reducing the lattice symmetry. One can identify this orientation by analyzing the anisotropy of the Zeeman splitting. For a spherically symmetric defect the Zeeman pattern of a bound exciton should be isotropic with small perturbations due to the cubic symmetry of the lattice.

In Fig. 3 we show PL spectra of the C line for $B=0$ T (c) and the Zeeman pattern for the C line in Voigt geometry for a polarization parallel (a) and perpendicular (b) to a (1,1,0) plane. The magnetic field has been rotated by 15° in the (1,1,0) plane from the [1,1,0] axis. The observed manifold of this Zeeman pattern with 28 magnetic subcomponents could not be explained with the common theory of bound excitons. Usually one expects six allowed transitions for bound excitons in high magnetic fields. For a detailed investigation the positions of the observed peaks as a function of angle of rotation have been plotted in Fig. 4.

The following conclusions can be drawn from these spectra. An electron-hole interaction mediates a specific mixing of electron and holes states. As a consequence even a small electron-hole interaction destroys the mirror symmetry of the Zeeman splitting.[10] It can be seen in Fig. 3 that there is a mirror symmetry of the Zeeman pattern with respect to the center of gravity of the line. Therefore, the electron-hole exchange interaction (H_{EX}) must

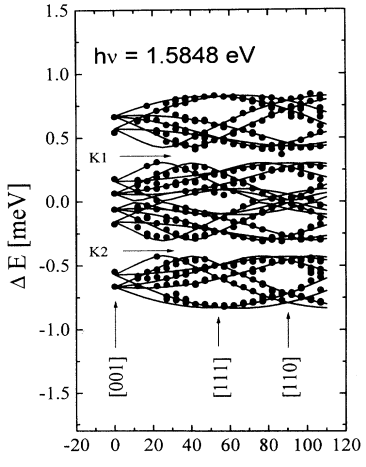

FIG. 4. Angular dependence of the Zeeman splitting of the C line subcomponents at $B=7.3$ T and $T=1.7$ K. The crystal was rotated in a [110] plane. $\mathbf{B}\|(0,0,1)$ is denoted by 0. The lines are calculated by simultaneous diagonalization of H [Eq. (1)]. The dots show the experimental data.

be negligibly small and not responsible for the unusually high number of magnetic subcomponents resolvable in the PL spectra [see Figs. 3(a) and 3(b)]. In addition, the diagmagnetic shift of the center of gravity (1.143×10^{-2} meV/T^2) allows the conclusion that the electron is weakly bound, and the local potential of this defect is predominantly attractive for holes.[11]

From the peak positions one can conclude that the orientation of the defect complex is close to the trigonal [1,1,1] axis, because **B**$\|$[1,1,1] led to the maximum Zeeman splitting. However, the trigonal site symmetry is broken. On the one hand one can recognize a large number of lines, and on the other hand a clear anticrossing of these lines for a range of energies identified as $K1$ and $K2$ in Fig. 4 is obvious. This can be understood only if we assume a symmetry lower than trigonal for the defect complex. In addition, for a pure trigonal complex symmetry only four magnetic subcomponents are allowed for **B**$\|$[0,0,1].

IV. PERTURBATION HAMILTONIAN

A. Cubic symmetry

As the explanation of the observed Zeeman pattern requires a model involving a Hamiltonian different from that used for bound excitons, up to now a closer inspection of symmetry reducing terms in the frame of an effective Hamiltonian will be given. Our considerations are restricted not only to isoelectronic traps, but also valid for any transition for which the initial and final states can be described with an effective Hamiltonian.

In spite of the fact that neutral defect complexes possess the same valence electron configuration as the atoms for which they substitute, some isoelectronic systems give rise to highly localized impurity states.[12] In 1965 Aten, Haanstra, and de Vries,[13] and independently Thomas, Hopfield, and Frosch[14] reported the optical properties of isoelectronic traps. Since then quite a large number of isoelectronic traps in semiconductors have been the subject of theoretical and experimental investigations. For a general review were refer to the paper of Czaja.[15] Most of these interaction traps are point defects. Defect complexes are isoelectronic only if the sum of the valence electrons in the defect complex is the same as the sum of valence electrons of the replaced host atoms.

The first principal considerations of an exciton bound to a neutral trap are related to the initial and final states. The angular momentum $J=0$ is attributed to this isoelectronic, final state (see Fig. 5). For the initial exciton states the angular momenta are $J=1$ and 2 coupled by the angular momenta of the electron $s=\frac{1}{2}$ and the hole $J=\frac{3}{2}$. In the case of a small crystal field, dipole transitions from the initial $J=2$ state to the final $J=0$ state are forbidden. But for a sufficiently strong, uniaxial field the distortion of the lattice removes the degeneracy of the $J=\frac{3}{2}$ hole state and the level splits into twofold-degenerate branches. The two $m_j=\pm1$ states of $J=1$ and 2 become mixed due to the transformation behavior of their wave functions, and then $m_j=\pm1$ for $J=2$ be-

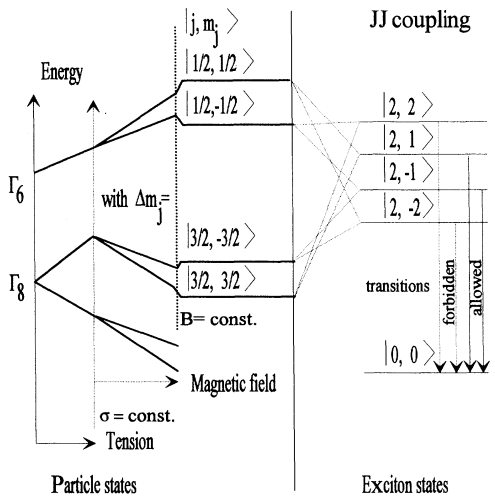

FIG. 5. Transition scheme of the electron Γ_6 and hole Γ_8 states in a strained cubic crystal. The perturbation due to the strain is much larger compared to the JJ splitting of the bound exciton. The degeneracy of the heavy and light holes is lifted because of the tension, but the degenerated Kramers doublets either the $|\frac{1}{2},\pm\frac{1}{2}\rangle$ Γ_6-electron states or the $|\frac{3}{2},\pm\frac{3}{2}\rangle$ and $|\frac{1}{2},\pm\frac{1}{2}\rangle$ Γ_8-hole states are splitted through a magnetic field only. The angular momenta of the hole $J=\frac{3}{2}$ and the electron $j=\frac{1}{2}$ couple to the exciton angular momenta $J=1$ and 2. For tensile strain the $J=2$ state possesses the lowest energy. This is the initial state for the exciton. The isoelectronic trap is labeled with the quantum number $J=0$. The second initial exciton state $J=1$ is probably due to the thermal depopulation not detectable.

comes an allowed transition. In an uniaxial crystal field the total angular momentum J is no longer a good quantum number. But the z component of the angular momentum m_j remains a constant of the motion. This z component is defined along the symmetry axis of the defect complex. We could not find emission from the upper state even for temperature $T=30$ K, where the C line is thermalized. Therefore the exciton state $J=1$ is supposed to be lifted by a relative strong crystal field into the conduction band.

The interpretation of the magnetooptical Zeeman data is performed by using a general perturbation Hamiltonian of cubic symmetry H,[16,17] modified by an additional term H_S, which we will explain and derive in Sec. II B. This Hamiltonian is based solely on symmetry considerations. The interpretation of the Zeeman data is therefore based on the symmetry of the exciton and the exciton binding defect. Its validity is not restricted to shallow impurities, for which the effective-mass approximation is valid. All known magnetic properties of an exciton up to the second order of magnetic field are well described by the following Hamiltonian:

$$H=H_{\mathrm{EX}}+H_{LB}+H_{QB}+H_S\ , \tag{1}$$

with the electron-hole exchange interaction

$$H_{EX}=-a\mathbf{J}\times\mathbf{S}-b(J_x^3\times S_x+J_y^3\times S_y+J_z^3\times S_z)\ , \quad (2)$$

the linear contribution of the magnetic field

$$H_{LB}=\mu_B[g_e\mathbf{S}\cdot\mathbf{B}+K\mathbf{J}\cdot\mathbf{B}+L(J_x^3B_x+J_y^3B_y+J_z^3B_z)]\ , \quad (3)$$

and the quadratic contribution of the magnetic field

$$H_{QB}=c_1B^2+c_2(\mathbf{J}\cdot\mathbf{B})^2+c_3(B_xB_y\{J_x,J_y\}+B_yB_z\{J_y,J_z\}+B_zB_x\{J_z,J_x\})\ , \quad (4)$$

where multis are used for direct products and the dots for dot products of vectors. μ_B is the Bohr magneton. The indices x, y, and z refer to the cubic axes of the lattice. J is the total angular momentum of the bound hole state.

B. Distortion

Magneto-optical data for bound excitons offer important information on the electronic structure; in particular, the symmetry of the complex can be deduced. Moreover, if the perturbation mechanism has a symmetry C_S which is lower than trigonal C_{3V}, the site symmetry can be investigated in the following way. The perturbation induced by the defect complex associated with the C line can be classified according to the irreducible representations of the crystal point group T_d. By using only linear combinations of the matrices associated with the irreducible representations Γ_1, Γ_3, and Γ_5 of T_d, we found the best fit for the angular-dependent Zeeman splitting. Therefore one can write H_S in the form

$$H_S=\begin{pmatrix} A & B & C & 0 \\ B^* & -A & 0 & C \\ C^* & 0 & -A & -B \\ 0 & C^* & -B^* & A \end{pmatrix}\ . \quad (5)$$

H_S describes an uniaxial distortion on a fourfold Γ_8 state. To obtain 28 eigenvalues by the simultaneous diagonalization of H, seven inequivalent sets of the constants A, B, and C are required. We found by a close inspection of H_S that the seven sets A, B, and C are correlated by all possible permutations of just three constants l, m, and n. For clarity we normalized $l^2+m^2+n^2=1$. Therefore we introduce two fitting constants D and W. Inserting the matrices of the suitable irreducible representations Γ_1, Γ_3, and Γ_5 of T_d, H_S is

$$H_S=-D[J_\zeta^2-\tfrac{1}{3}J(J+1)]-W[lm\{J_x,J_y\}+ln\{J_x,J_z\}+nm\{J_y,J_z\}]\ , \quad (6)$$

with $J_\zeta=(lJ_x+mJ_y+nJ_z)$.

This modified Hamiltonian H has led to an excellent agreement with the observed data. The fitting parameters are listed in Table II. The C line is interpreted as a superposition of bound exciton recombinations from several inequivalent sets of distortions described by H_S. With this form of H_S for $B=0$ T, all 28 eigenvalues are degenerate as observed in the experiment.

We will show that a perturbation Hamiltonian derived for an external uniaxial strain in arbitrary direction $[l,m,n]$ is identical to H_S. Thus for the defect complex associated with the C line we established a model of a strain-inducing defect in a homogeneous lattice. With this model it is possible to explain the change of the C line by aging as a destruction of the homogeneity, which starts from the sample surfaces. For very thin MBE-grown CdTe films, after some weeks the homogeneity around the defect complexes is removed and the C line in the PL spectrum is no longer detectable.

For neutral (isoelectronic) traps the change in potential energy caused by the misfit associated with isoelectronic traps[12] is responsible for the capture of a charged particle. This assumption is supported by the fact that isoelectronic traps inside the band gap have been found only when the impurity center is either very large [for instance GaP:Bi (Ref. 18)] or very small [GaP:N (Ref. 14)]. As a consequence, the magneto-optical data for excitons bound to isoelectronic traps indicate in most cases a reduction of the site symmetry T_d of the host crystal in the neighborhood of the defect to trigonal C_{3V} symmetry.

Assuming a point defect in a homogeneous lattice one cannot distinguish whether the lattice in the recombination area is strained by an external force or by the intrinsic defect; the derivation of a symmetry reducing Hamiltonian describing a strain is straightforward. Furthermore this concept is compatible with the assumption that the wave function of the hole is sufficiently located around the lattice deformation. This model of the bound exciton is equivalent with the Hopfield-Thomas-Lynch model[19] of an isoelectronic trap. Rapidly disappearing forces, which decay much faster than Coulomb forces, are mainly responsible for the local trapping of charged particles, especially holes. By the localization the wave function has become modulated. The range of such a potential is very small, and of the order 1 Å.[20] A second particle with opposite size can be bound by Coulomb interaction, and consequently the exciton recombination occurs at the center of the disturbance.

For the theory of magneto-optical phenomena the transformation behavior of a defect complex is significant. Around a defect a modification is produced by the lattice relaxation due to the size difference between the complex and the host atoms.[12] Two types of relaxation mechanisms have been discussed in conjunction with isoelectronic traps. The first one arises geometrically from the substitution of a lattice atom with a neutral dopant, the second originates from the stationary charge distribution of the trapped electronic particles. For a hole-attracting trap the wave function is mainly p like. But the s- and p-like terms of the isoelectronic potential can cause some changes in the K or L factors of the Hamiltonian describing the exciton in Eq. (3). Both aspects apply here, but the small deviation from the typical value $K=0.6$ (Ref. 21) indicates that the deformation part dominates. In any way, the misfit due to the introduction of dopants will strain the crystal lattice structure. Within a linear approximation, the change in the potential energy due to the strain is

$$V=V_{xx}\varepsilon_{xx}+V_{yy}\varepsilon_{yy}+V_{zz}\varepsilon_{zz}+2(V_{yx}\varepsilon_{yz}+V_{zx}\varepsilon_{zx}+V_{xy}\varepsilon_{xy})\ , \quad (7)$$

where: $\varepsilon_{ij}=\frac{1}{2}[(\partial u_i/\partial x_j)+(\partial u_j/\partial x_i)]$ is the strain tensor and $u(\mathbf{r})$ is the displacement due to the stress at the point $\mathbf{r}$. Obviously V is a symmetry tensor. By using the method of combination of the irreducible representations of T_d with the decompositions of the strain tensor, we obtain the following term, which reduces the cubic symmetry.[22] A review and a detailed discussion of this method can be found in the paper by Rodriguez, Fisher, and Barra.[23] After some algebraic manipulation we obtain Eq. (7) in the following form. It deviates somewhat from the usual form; for convenience the factor 2 in the third term of Eq. (3) was put in the denominator:

$$V=aI(\varepsilon_{xx}+\varepsilon_{yy}+\varepsilon_{zz}) +b[\varepsilon_{xx}(J_x^2-\tfrac{5}{4}I)+\varepsilon_{yy}(J_y^2-\tfrac{5}{4}I)+\varepsilon_{zz}(J_z^2-\tfrac{5}{4}I)] +\frac{d}{2\sqrt{3}}(\varepsilon_{yz}\{J_y,J_z\}+\varepsilon_{zx}\{J_z,J_x\}+\varepsilon_{xy}\{J_x,J_y\}) , \quad (8)$$

where I is the unit 4×4 matrix, and the anticommutator $\{A,B\}=AB+BA$. J_x, J_y, and J_z are the matrix operators corresponding to total angular momentum of the hole $J=\frac{3}{2}$. We choose the form given by Luttinger[16] with diagonal J_z:

$$J_x=\frac{i}{2}\begin{pmatrix}0&\sqrt{3}&0&0\\-\sqrt{3}&0&2&0\\0&-2&0&\sqrt{3}\\0&0&-\sqrt{3}&0\end{pmatrix},\quad J_y=\frac{1}{2}\begin{pmatrix}0&\sqrt{3}&0&0\\\sqrt{3}&0&2&0\\0&2&0&\sqrt{3}\\0&0&\sqrt{3}&0\end{pmatrix},\quad J_z=\frac{1}{2}\begin{pmatrix}3&0&0&0\\0&1&0&0\\0&0&-1&0\\0&0&0&-3\end{pmatrix}. \quad (9)$$

To describe the internal state of stress induced by the defect complex we considered a purely normal traction through the point of maximum stress.[24] Because of the sharpness of the C line we neglect any stress gradient, which contributes to a broadening of the C line. Combining the strain tensor with the stress components we find an ansatz referred to arbitrary axes x, y, and z:

$$(\sigma_{xx},\sigma_{yy},\sigma_{zz},\sigma_{yx},\sigma_{zx},\sigma_{zy})^T =\sigma(ll,mm,nn,ml,nl,nm)^T , \quad (10)$$

where $[l,m,n]$ is the direction of the stress and σ its magnitude. If the $\mathrm{sgn}(\sigma)>0$ the stress is a tension; otherwise it is a pressure. Proper representations for these directions are spherical coordinates: $l=\sin\vartheta\cos\varphi$, $m=\sin\vartheta\sin\varphi$, and $n=\cos\vartheta$. For small displacements Hooks' law is a valid approach. The dependence between the strain tensor and the stress for a cubic lattice is given by[25]

$$\begin{pmatrix}\varepsilon_{xx}\\\varepsilon_{yy}\\\varepsilon_{zz}\\2\varepsilon_{yz}\\2\varepsilon_{zx}\\2\varepsilon_{xy}\end{pmatrix}=\begin{pmatrix}S_{11}&S_{12}&S_{12}&0&0&0\\S_{12}&S_{11}&S_{12}&0&0&0\\S_{12}&S_{12}&S_{11}&0&0&0\\0&0&0&S_{44}&0&0\\0&0&0&0&S_{44}&0\\0&0&0&0&0&S_{44}\end{pmatrix}\begin{pmatrix}\sigma_{xx}\\\sigma_{yy}\\\sigma_{zz}\\\sigma_{yz}\\\sigma_{zx}\\\sigma_{xy}\end{pmatrix} \quad (11)$$

where S_{ij}'s are the system and defect specific elastic coefficients. For an external strain in CdTe typical values derived from piezomodulation measurements[26] are given in Table I.

In the frame of an effective Hamiltonian a shift in energy is insignificant. Therefore, we will neglect all shifted parts in V [Eq. (8)]. After some mathematical procedures, inserting Eqs. (11) and (10) into Eq. (8) and transposing this equation for clarity, we obtain

$$H_S=V-\sigma\underline{\frac{aI}{\text{shift}}};$$

in the same form as derived in Eq. (6), when we exploited the correlations of the seven sets A, B, and C in Eq. (5).

The constants D and W are dependent on deformation potentials b and d. For a uniaxial strain, one can find the following relations:

$$D=b\sigma(S_{12}-S_{11}) ,$$

$$W=b\sigma(S_{11}-S_{12})-\frac{d}{4\sqrt{3}}\sigma S_{44} .$$

Some interesting properties of H_S should be mentioned. If the total CdTe crystal is uniaxially strained, the ratio W/D important for the theoretical fitting should be in the range of -0.57 (calculated with the parameters in Table I). For trigonal planar strain the constant D should be 0. Each deviation from this indicates an exciton binding system different from the host lattice CdTe, in our case a defect complex. Using H_S it is now possible

TABLE I. Typical values for bulk CdTe deformation potentials and elastic coefficients evaluated by piezomodulation (Ref. 19).

Hydrostatic: a (eV)	Tetragonal: b (eV)	Trigonal: d (eV)	S_{11} (10^5 MPa^{-1})	S_{12} (10^{-5} MPa^{-1})	S_{44} (10^{-5} MPa^{-1})
-3.27	1.15 ± 0.02	3.36 ± 0.10	3.581	-1.394	5.1

to simulate all simple strain directions of complexes, which have captured an exciton. For most isoelectronic traps the trigonal [1,1,1] axis will be the direction of the strain, and H_S could be written as in previous publications. For this special case where $l=m=n=1/\sqrt{3}$, the symmetry is reduced to C_{3V}, and we obtain the common form of H_S:[10,27]

$$H_S=-\frac{(D+W)}{D}[J_\zeta^2-\tfrac{1}{3}J(J+1)]\ . \tag{12}$$

The II-VI semiconductor CdTe shows a rather large piezoelectric effect. But here the anisotropy of the Zeeman pattern observed by rotation of the magnetic field is not caused by an internal electric field. The influence of an electric field $\mathbf{E}=|\mathbf{E}|(l_E,m_E,n_E)^T$ on the Γ_8-hole state with angular momentum $J=\frac{3}{2}$ has been taken into account by using H_S for $D=0$ (Ref. 28) and the substitutions $l_E=lm$, $m_E=ln$, and $n_E=nm$. Applying this Hamiltonian the effect of an electric field on the anisotropy of the Zeeman splitting of the C line turned out to be negligible.

Strain can never cause a splitting in Kramers' doublets, for instance, in a Γ_8 conduction band. It is shown schematically in Fig. 5 that such a degeneracy can be lifted by magnetic fields only. Under the assumption that for the unperturbed Hamiltonian the spin-orbit interaction is the dominating effect, while the strain-induced symmetry lowering of the crystal field is the main part in the perturbed Hamiltonian, in our formalism we used a basis set of two twofold-degenerate hole states $|\frac{3}{2},\pm\frac{3}{2}\rangle$ and $|\frac{3}{2},\pm\frac{1}{2}\rangle$. The lowest-energy state is $|\frac{3}{2},\pm\frac{3}{2}\rangle$ if the local strain field is tensional.

Therefore, a 4×4 matrix representation for the Γ_8 valence band with the angular momentum $J=\frac{3}{2}$ the perturbation Hamiltonian H_S has the form

$$H_S=\begin{bmatrix} -\frac{1}{4}D[3(l^2+m^2)+9n^2-5] & -\sqrt{3}(D+W)(mn+i\ln) & -\frac{\sqrt{3}}{2}(D+W)(m+il)^2 & 0 \\ -\sqrt{3}(D+W)(mn-i\ln) & -\frac{1}{4}D[7(l^2+m^2)+n^2-5] & 0 & -\frac{\sqrt{3}}{2}(D+W)(m+il)^2 \\ -\frac{\sqrt{3}}{2}(D+W)(m-il)^2 & 0 & -\frac{1}{4}D[7(l^2+m^2)+n^2-5] & -\sqrt{3}(D+W)(-i\ln-mn) \\ 0 & -\frac{\sqrt{3}}{2}(D+W)(m-il)^2 & -\sqrt{3}(D+W)(i\ln-mn) & -\frac{1}{4}D[3(l^2+m^2)+9n^2-5] \end{bmatrix}. \tag{13}$$

The theoretical fit depicted with straight lines in Fig. 4 has been computed by simultaneous diagonalization of all terms in Eq. (1).

V. DISCUSSION

The interpretation of the best-fitting constants of H (Table II) with our model of the defect will be given in this section. Obviously the ratio $W/D=-1.1$ is far away from the ratio $W/D=-0.56$ expected for an external force. Thus we can exclude a long-range tensile deformation in the CdTe samples. The ratio $W/D=-1.1$ is to our knowledge, the first experimentally supported indication for an intrinsic, strain-inducing defect. Furthermore, we find that the cubic symmetry of the CdTe crystal in the neighborhood of the defect is reduced to a symmetry lower than trigonal because of strong tensional forces caused by an isoelectronic trap and not by an internal electric field. Otherwise the constant D should be zero. In addition to that, all terms of the Hamiltonian estimating cubically symmetric interactions caused by the electron-hole-exchange interaction [Eq. (2)] and the wave function of the hole [which is related to the constant L in Eq. (3)] have been found to be negligibly small.

For some directions of the magnetic field we found up to 28 peaks in the photoluminescence spectra for polarizations parallel and perpendicular to a [1,1,0] axis, which are degenerate in the C line with a half-width of 0.12 meV without magnetic field.

Our model of the complex has to meet the following requirements: (1) Indium atoms and cadmium vacancies

TABLE II. These parameters of the Hamiltonian [Eq. (1)] describe the Zeeman splitting of the indium-related 1.584 19-eV luminescence.

g	a (meV)	b (meV)	K	L	c_1 (meV/T^2)	c_2,c_3 (meV/T^2)	W/D
-1.73 ± 0.03	0.0 ± 0.02	0.0 ± 0.02	0.75 ± 0.03	0.0 ± 0.03	1.143×10^{-2}	0.0	-1.10 ± 0.05
ϑ	φ		$l=\cos\varphi\sin\vartheta$		$m=\sin\vartheta\sin\vartheta$		$n=\cos\vartheta$
52.7	45.0		0.56 ± 0.01		0.56 ± 0.01		0.61 ± 0.01

are constituents of the trap. (2) In addition to that, the complex must be isoelectronic. (3) The main direction of strain is the trigonal [1,1,1] axis, with a small inclination toward a Cartesian axis. Our model of the defect is an isoelectronic In_{Cd}-V_{Cd}-In_{Cd} complex, which is strained in such a way that the complex is tilted by an angle of $\tau=2°$ from the [1,1,1] orientation. To determine the microscopic nature of the complex we have to distinguish between a linear trap with a trigonal orientation and a complex consisting of close neighbors. The first one is inconsistent, because the large number of atoms inside the complex to be postulated is unrealistic. According to our results the complex consists of three nearest neighbors in a plane with a normal vector in [1,1,1] direction. The two indium atoms and the cadmium vacancy form a triangle, as sketched in Fig. 6. This small complex causes a displacement of the next neighbors, resulting in a tensile strain. Due to the fact that indium atoms are quite small compared to cadmium atoms, for which they substitute, the normal vector of the defect plane is tilted toward the cadmium vacancy. As a result, the strain in the plane In_{Cd}-V_{Cd}-In_{Cd} with a normal vector [1,1,1] leads to a simple tension in the [1,1,1] direction with a small inclination τ toward the Cartesian axis. This complex causes a tensionally strained lattice in the neighborhood of the defect.

The angle of inclination $\tau=2°$ with an estimated error of $\pm 0.5°$ was determined from the anticrossing in the areas $K1$ and $K2$ shown in Fig. 4. The theoretical fit is very sensitive to changes in τ. For instance, there is no anticrossing for $\tau=0°$ anymore.

A consequence of our microscopic model of an In_{Cd}-V_{Cd}-In_{Cd} complex is that an A-center-like D_{Cd}-V_{Cd} complex (D is a donor on a cadmium site like aluminum or indium) leads to a tetragonal symmetry consistent with recent optically detected magnetic resonance measurements by Stadler *et al.*[29] In an alternative model for the C-line complex Zimmermann *et al.*[8] suggest that the nearest neighborhood of the complex consists of an interstitial indium and a cadmium vacancy plus a single ionized acceptor. With this proposal for the C-line complex it is not possible to explain the improvement of the carrier mobility after doping the samples with an excess of cadmium.[2] These authors made also magneto-optical measurements on an indium-related luminescence line, but they were not able to resolve the magnetic subcomponents. By fitting the shape of a line with a half-width more than five times larger than ours, they suggest a trigonal complex center with different g factors for the hole. They also applied the unmodified Hamiltonian,[10,27] and were therefore not able to find any off-trigonal complex symmetry. As mentioned above, the C-line luminescence degrades with time, resulting in a broadening of the line caused by complexes in different relaxed states, which probably averaged over all off-trigonal axes leading to a pure trigonal complex symmetry.

The high number of magnetic subcomponents observed in this work can be explained in the following way. In a cubic lattice there exist eight [1,1,1] axes. In the range of each of these trigonal axes there are three possibilities to tilt the complex axis towards the Cartesian axes. Without magnetic field the electronic structure of a bound exciton trapped by a defect oriented along these

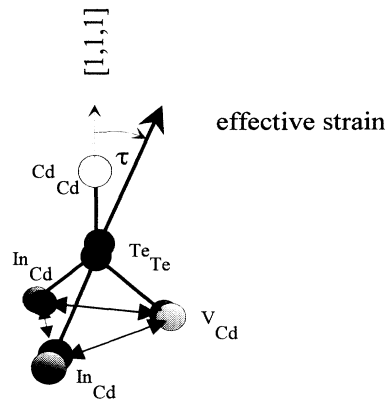

FIG. 6. The atomic model of the isoelectronic trap consists of In_{Cd}-V_{Cd}-In_{Cd} complex in a plane with the normal vector in (1,1,1) direction. As the indium atoms are not equivalent to the cadmium vacancies, the simple tension describing the normal vector is tilted toward a Cartesian axis with an angle $\tau=2$. This model predicts a tetragonal symmetry reduction for an A-center-like complex in the (1,1,0) direction.

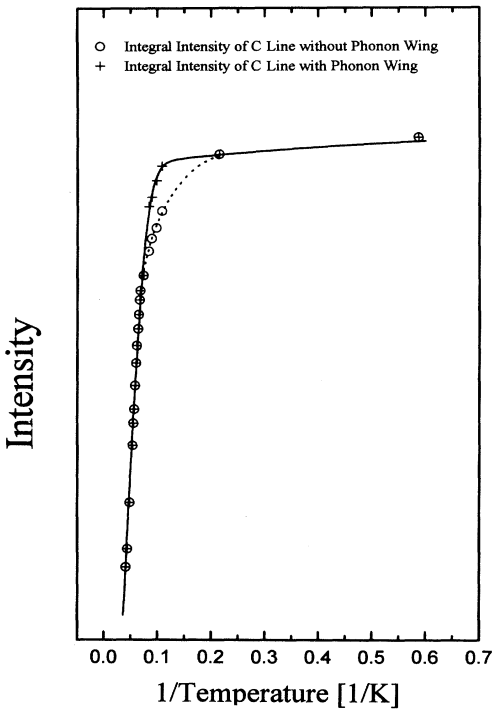

FIG. 7. The integral intensities of the C-line photoluminescence with the continuous phonon sideband (crosses) and without (circles) is plotted as a function of the reciprocal temperature. The temperature was varied in the range between $T=1.7$ and 35 K. For the lowest temperature $T=1.7$ K the two intensities are normalized to each other.

directions is degenerate, but for directions of the magnetic field oriented in a (1,1,0) plane for several of these 8×3 axes, the degeneracy is lifted. Considering the possible eigenvalues of H [Eq. (1)] describing the magnetic subcomponents of the C line, one can find that different axes of distortion contribute to four different eigenvalues only, whenever the projection of these axes on the (1,1,0) plane are distinguishable. All three possible inclinations of eight trigonal axes toward the three Cartesian axes result in just seven different projections on a (1,1,0) plane. Therefore the seven sets of constants A, B, and C are connected with these seven different projections. This is an additional hint that the small inclinations for the trigonal [1,1,1] axes are not randomly oriented; on the contrary, all defect complexes are incorporated with same site symmetry C_s. This directional degeneracy is also the reason why the Zeeman spectra of the C line with a magnetic field along the [1,1,0] axis for polarizations parallel and perpendicular to a (1,1,0) plane are not distinguishable.

The interpretation of the C line as a superposition of bound exciton recombinations associated with 8×3 configurations of the defect complexes is also consistent with the observation that, even for high magnetic field (see Fig. 3), the lines are still symmetric about the center. With a lattice temperature of 1.7 K ($\approx$0.2 meV) when the Zeeman splitting of the C line is approximately 2 meV the line intensities are not related by Boltzmann factors. Each magnetic subcomponent in the spectra thus comes from a separate class of defects. If the excitons are strongly confined to these defects then they become thermally uncoupled.

VI. TEMPERATURE DEPENDENCE OF THE C LINE

The C line always is accompanied by a low-energy phonon sideband (Figs. 1 and 2) with a maximum at the 4.3-meV TA(X) phonon.[30] The coupling of the C line to its acoustical-phonon replica is stronger compared to those of acceptor bound excitons. For some MBE samples the intensity of the phonon wing maxima is in the range of the no-phonon C line. In the case of donor bound excitons in CdTe these replicas are negligibly small. We suggest that the non-Coulomb-like, rapidly disappearing forces of an isoelectronic defect complex support the acoustical, non-dipole-like vibrations of the lattice. In the In_{Cd}-V_{Cd}-In_{Cd} plane the equivalent direction of vibration for this complex, which is tilted towards the Cartesian axes, will be a [1,0,0] direction. In this direction the next neighbor is a cadmium atom (see Fig. 6). Thus the TA(X) phonon couples rather tightly and leads to a maximum distance for the phonon sideband.

The strain-related behavior of this complex and, particularly, the coupling to the acoustical phonons, is confirmed by the temperature dependence of the C-line intensity. In Fig. 7 we have plotted the integral intensity of the C line with (crosses) and without (circles) the phonon sideband normalized for the lowest temperature $T=1.7$ K. This behavior of the bound exciton emission intensity with temperatures from 1.7 up to 35 K gives additional information about the phonon coupling. We observe a lowering in the normalized no-phonon C-line intensities for the temperature range between 4.2 and 15 K. Obviously, if the vibration energy due to the increase in temperature is in the range of the acoustical-phonon energies, the coupling of the electronic transition to low-energy acoustic phonons is the dominating quenching effect of the C-line luminescence.

The tensional forces connected with the isoelectronic traps enhance the emission of phonons. As a consequence, a strong phonon sideband is detectable. We observed this phenomenon for many strain-inducing defects. For many MBE-grown CdTe samples the intensity of the TA(X) phonon is almost equal to the intensity of the no-phonon line if the lattice is strained by the defect. The phonon side wing obviously is a hint for a strained lattice in the vicinity of the trap. Details for different lines will be published elsewhere.

The thermal quenching of the C-line intensities has been fitted according to a theory of Bimberg, Sondergeld, and Grove.[31] The best results for total integrated emission intensity (solid line in Fig. 7) was fitted with one activation energy of $E=7.6$ meV for higher temperatures. As the binding energy of a free exciton in CdTe is about 10 meV, the observed activation energy of 7.6 meV agrees very well with the dissociation of free excitons. Therefore, we suggest that the activation energy $E=7.6$ meV can be attributed to the second excited state of the bound exciton.

To describe thermal quenching of the C line, a second activation energy of 1.2 meV has been determined (dotted line in Fig. 7). This energy is interpreted as a phonon energy describing the electron-phonon coupling.

VII. CONCLUSIONS

Photoluminescence measurements in external magnetic fields have been employed to identify the symmetry, microscopic structure, and chemical origin of a defect complex that binds an exciton resulting in a luminescence line at 1.584 19 eV, commonly referred to as the C line. From the investigation of the C-line intensity as a function of the MBE growth conditions, we identify indium atoms and cadmium vacancies as constituents of the complex. As no acceptor-related recombinations correlated with the C line can be observed, we identify the complex as isoelectronic. This identification is further confirmed by the drastic increase of the carrier concentration by MBE growth under additional cadmium flux.

By investigation of the anisotropy of the Zeeman splitting we have deduced the electronic character and microscopic structure of this indium-related defect associated with the C-line luminescence. The experimental data are in excellent agreement with the numerical data obtained in the frame of a perturbation Hamiltonian using the parameters listed in Table II.

The modified effective Hamiltonian presented in this paper applicable for arbitrary directions of the strain reduces to the well-known operators of bound excitons with cubic T_d trigonal C_{3V}, or tetragonal C_{2V} symmetries. By using this Hamiltonian we have analyzed in

detail the electronic structure of the isoelectronic complex associated with the C line.

The defect complex is formed of a strained planar triangle In_{Cd}-V_{Cd}-In_{Cd}, where the strain axis is tilted by a small angle of 2° with respect to the [1,1,1] axes in the direction of the Cartesian axes. Due to the fact that the defect complex In_{Cd}-V_{Cd}-In_{Cd} does not fit into the host-lattice structure, the intrinsic defect is not oriented along the trigonal [1,1,1] axis but slightly inclined.

Close to the sample surface no balance exists between the strain forces caused by the defect and the lattice. As a consequence the defect axis will eventually relax, resulting in a broadening of the half-width of the C line. This relaxation starts at the surface and migrates into the sample with time. This explains why the C-line luminescence broadens by a factor of 5 within six months. If the surface of the sample is etched, the C line becomes narrow again with a half-width of 0.12 meV.

From the magneto-optical measurements we have deduced that the electron of the exciton is bound weakly to an acceptorlike isoelectronic defect. In the frame of an isoelectronic defect model with pronounced strain in the neighborhood, non-Coulomb forces should lead to a strong coupling of the electronic states to the branch of acoustical phonons resulting in an intense phonon sideband. Our temperature-dependent measurements of the integral C-line luminescence show this strong phonon coupling, again confirming the model of a strain-inducing, isoelectronic defect complex.

ACKNOWLEDGMENTS

The authors would like to thank Professor A. Ramdas and Professor S. Rodriguez for useful suggestions, and the Deutsche Forschungsgemeinschaft for financial support. One of us (L.W.) is grateful for a fellowship granted from Cusanuswerk.

[1]B. Monemar, E. Molva, and L. S. Dang, Phys. Rev. B **33**, 1134 (1986).

[2]W. Ossau, T. A. Kuhn, A. Hauck, D. Hommel, A. Waag, S. Scholl, G. Landwehr, and D. Sinerius, in *Proceedings of the 21st International Conference on the Physics of Semiconductors, Beijing, 1992,* edited by P. Jiang and H.-Z. Zheng (World Scientific, Singapore, 1992), Vol. II, 1963.

[3]P. J. Dean, Phys. Rev. B **4**, 2596 (1971).

[4]L. Worschech, W. Ossau, and G. Landwehr, in *Proceedings of the 22nd International Conference on the Physics of Semiconductors, Vancouver, 1994,* edited by D. J. Lockwood (World Scientific, Singapore, 1994), Vol. I, p. 333.

[5]Z. C. Feng, M. G. Burke, and W. J. Choyke, Appl. Phys. Lett. **53**, 128 (1988).

[6]C. E. Barnes and K. Zanio, J. Appl. Phys. **46**, 3959 (1975).

[7]N. C. Giles, R. N. Bicknell, R. L. Harper, S. Hwank, K. A. Harris, and J. F. Schetzina, J. Cryst. Growth **86**, 348 (1988).

[8]H. Zimmermann, R. Boyn, M. U. Lehr, H.-J. Schulz, P. Rudolph, and J.-Th. Kornack, Semicond. Sci. Technol. **9**, 1598 (1994).

[9]E. Molva and J. L. Pautrat, Solid State Commun. **39**, 1151 (1981).

[10]W. M. Chen, Q. X. Zhao, B. Monemar, H. P. Gislason, and P. O. Holtz, Phys. Rev. B **35**, 5722 (1986).

[11]H. P. Gislason, B. Monemar, Z. G. Wang, C. Uihlein, and P. L. Liu, Phys. Rev. B **32**, 3723 (1985).

[12]A. Baldereschi, J. Lumin. **7**, 79 (1973).

[13]A. C. Aten, J. H. Haanstra, and H. de Vries, Philips Res. Rep. **20**, 395 (1965).

[14]D. G. Thomas, J. J. Hopfield, and C. J. Frosch, Phys. Rev. Lett. **15**, 857 (1965).

[15]W. Czaja, in *Festkörperprobleme,* edited by O. Madelung (Vieweg, Braunschweig, 1971), Vol. XI.

[16]J. M. Luttinger, Phys. Rev. **102**, 1030 (1956).

[17]B. Monemar, P. O. Holtz, W. M. Chen, H. P. Gislason, and U. Lindefelt, Phys. Rev. B **34**, 8656 (1986).

[18]F. A. Trumbore, M. Gerhenzon, and D. G. Thomas, Appl. Phys. Lett. **9**, 4 (1966).

[19]J. J. Hopfield, D. G. Thomas, and R. T. Lynch, Phys. Rev. Lett. **17**, 312 (1966).

[20]D. R. Penn, Phys. Rev. **128**, 2093 (1962).

[21]W. Ossau, T. A. Kuhn, and R. N. Bicknell-Tassius, J. Cryst. Growth **101**, 135 (1990).

[22]G. L. Bir and G. E. Pikus, *Symmetry and Strain-Induced Effects in Semiconductors* (Wiley, New York, 1974).

[23]S. Rodriguez, P. Fisher, and Fernando Barra, Phys. Rev. B **5**, 2219 (1972).

[24]A. E. H. Love, *A Treatise on the Mathematical Theory of Elasticity* (Dover, New York, 1944), p. 81.

[25]C. Kittel, *Festkörperphysik* (Wiley, Frankfurt, 1973).

[26]E. Kurtz, H. J. Lugauer, D. Hommel, A. Waag, and G. Landwehr (unpublished).

[27]H. P. Gislason, B. Monemar, P. O. Holtz, P. J. Dean, and D. C. Herbert, J. Phys. C **15**, 5467 (1992).

[28]A. Abragam and B. Bleaney, *Electron Paramagnetic Resonance of Transition Ions* (Clarendon, Oxford, 1970).

[29]W. Stadler, B. K. Meyer, D. M. Hoffman, B. Kowalski, P. Emanuelsson, P. Omling, E. Weigel, C. Müller-Vogt, and R. T. Cox, Mater. Sci. Forum **143-147**, 399 (1994).

[30]J. M. Rowe, R. M. Nicklow, D. L. Price, and K. Zanio, Phys. Rev. B **10**, 671 (1974).

[31]D. Bimberg, M. Sondergeld, and E. Grobe, Phys. Rev. B **4**, 3451 (1971).

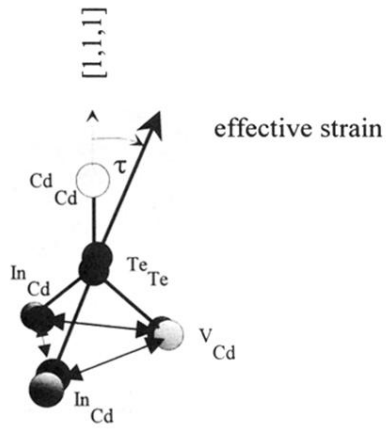

FIG. 6. The atomic model of the isoelectronic trap consists of In_{Cd}-V_{Cd}-In_{Cd} complex in a plane with the normal vector in (1,1,1) direction. As the indium atoms are not equivalent to the cadmium vacancies, the simple tension describing the normal vector is tilted toward a Cartesian axis with an angle $\tau=2$. This model predicts a tetragonal symmetry reduction for an *A*-center-like complex in the (1,1,0) direction.